v. 3, n. 24, 2023

Journal of
Engineering
Research

SHALLOW GAS ACCUMULATION IN SEDIMENTS FROM THE NORTH TERMINAL OF THE PORT OF AVEIRO, RIA DE AVEIRO, PORTUGAL

Laurício Corrêa Terra
Geosciences Department and CESAM, University of Aveiro

Luis Menezes Pinheiro
Geosciences Department and CESAM, University of Aveiro

Ricardo Correia
Geosciences Department and CESAM, University of Aveiro

Abstract: In this work, we report evidence of shallow gas accumulations in sediments and escape in the water column, discovered and mapped in the North Terminal of the Port of Aveiro, using high resolution seismic data (Chirp Sonar). This evidence includes: Acoustic Turbidity in the subsurface and Acoustic Plumes in the water. Two high resolution seismic and sediment sampling campaigns were carried out in this area, separated by 5 years, to analyze gas field evolution. In the first campaign (2013) a gas field with an area of 0.22Km² was mapped. In the second campaign (2018) the same field showed a total area of approximately 0.34 km², suggesting an increase in the area of gas accumulations. The seismic stratigraphic analysis of the high-resolution seismic profiles showed three main seismo-stratigraphic units: Unit U1, consisting of marls, clays and limestones from the Upper Cretaceous, and Units U2 and U3, composed of sediments (sands and clays) from the Quaternary (Plio-Pleistocene and Holocene). The gas accumulations were found in the Quaternary sediments. The gas is inferred to be of biogenic origin, resulting from the degradation of the accumulations of organic matter deposited by river channels from the sea regression after the last glacial maximum.
Keywords: Shallow gas, high-resolution seismic, estuary, Ria de Aveiro

INTRODUCTION

Coastal barrier/lagoon systems are of high environmental and economic importance, particularly when artificially permanently connected to the sea and when they host harbor facilities, as is the case of the Ria de Aveiro. The knowledge about the geological processes governing the evolution of such coastal systems is essential for the management of its natural resources, for the evaluation of the risk of geological hazards and to provide knowledge for environmental impact studies related to recurring dredging operations required for harbor maintenance and expansion.

These systems are depocenters of organic-rich sediments (Kelley et al., 1995; Van der Nat and Middelburg, 2000) and form excellent easily accessible natural laboratories to investigate the mechanisms of natural gas generation, accumulation, migration and escape (e.g., Garcia-Gil, 2003). In these regions, continental discharge and local biological contribution support the deposition and accumulation of organic matter in the fine sediments, which generates gas via its degradation.

Methane is an important greenhouse gas, being the most abundant hydrocarbon in the atmosphere (Zhou et al., 2009) and therefore representing a major contributor to climate change. It can represent a problem for geotechnical stability for underwater operations, but it may represent an opportunity as an alternative energy source.

Gas accumulations in shallow shelf and coastal sediments are a common phenomenon worldwide (e.g., Park et al., 1991; Karisiddaiah et al., 1992; Papatheodorou et al., 1993; Garcia-Garcia et al., 1999, 2007; Okyar and Ediger, 1999; Fleischer et al., 2001; Missiaen et al., 2002; Garcia-Gil, 2003; Duarte et al., 2007; Martínez-Carreño and Garcia-Gil, 2013; Terra, 2014; Weschenfelder et al, 2016).

The presence of gas in marine sediments can originate from either biogenic or thermogenic processes (Floodgate and Judd, 1992), but the most common gas in shallow-water sediments is biogenic and is produced by microbial methanogenesis under anaerobic conditions (Judd and Hovland, 2007). The various gas sources and modes of accumulation are closely related to the sedimentary and evolutionary processes occurring in the coastal depositional environment (Garcia-Gil et al., 2002). Sandy

packages may form gas reservoirs, while the finer, mainly muddy sediments form sealing layers.

The acoustic responses caused by the presence of shallow gas in seismic records has various distinct characteristics and can be revealed by acoustic blanking, acoustic turbidity, enhanced reflections, acoustic columns, intra-sedimentary plumes, and acoustic plumes in the water layer (Hovland and Judd, 1988; Iglesias and García-Gil, 2007; Judd and Hovland, 2007; Lee et al., 2005; Missiaen et al., 2002; Schroot and Schüttenhelm, 2003).

In this work we show the results from two high resolution seismic refection surveys (Chirp sonar), separated by a time lapse of 5 years, that were conducted in the North Terminal of the Port of Aveiro, in the Ria de Aveiro barrier/lagoon system (Portugal), to map and investigate the evolution of the gas accumulations first revealed by acoustic anomalies in 2013.

GEOGRAPHICAL AND GEOLOGICAL SETTING OF THE RIA OF AVEIRO

The Ria de Aveiro is a fairly recent barrier-lagoon system (only a few centuries), located along the northwest Portuguese coast (Figure 1). This system covers an area of approximately 530 km² and is located at the mouth of a drainage basin of 3 635 km² (the Vouga river and its tributaries). The tidal regime is semi-diurnal with an average amplitude of 1.90 meters and a maximum around 2.57 meters during spring tides (Duarte et al., 2007). The phase lag, variable at high and low water, increases upstream up to 5h, with low and high tides sometimes occurring simultaneously in different parts of the lagoon (Dias et al., 2000).

As concerns geology, the consolidated lagoon bedrock of Mesozoic age (Upper Cretaceous) is cut by a marine ravinement surface that dips gently westwards (less than 1º) and by an older fluvial erosion surface probably dating from the last glacial maximum, 18Ky BP (Duarte et al., 2007). The coastal and lagoon recent sediments are essentially unconsolidated dune, beach, barrier and lagoon sands and clays, deposited during the Pleisto-Holocene transgression and highstand. Elevated sand and gravel beach deposits from prior Quaternary cycles are described inland, where they outcrop (Teixeira and Zbyszewski, 1976). The Quaternary sedimentary sequence lays unconformably over the Mesozoic sedimentary succession of clays, marls and limestones of the Lusitanian basin, that dip to the west, deposited during the opening of the Atlantic. Locally, the lower boundary of the Quaternary sediments fills paleo channels cut through the Mesozoic clays, marls and limestones (the so-called "Aveiro Clays", of Upper Cretaceous age).

Direct observations of escape of biogenic methane from several boreholes in Quaternary sediments from the area surrounding the Ria of Aveiro were reported for the first time by the Portuguese Geological Survey in 1967 (Faria et al. 1967). Duarte et al. (2003) identified some of these features correspond to pockmarks. More recently, Duarte et al. (2007) identified evidence of extensive gas accumulation and seepage in tidal channel sediments from the Ria de Aveiro barrier lagoon.

DATABASE AND METHODS

GEOPHYSICAL DATA

Two geophysical surveys were carried out in the study area, in 2013 and 2018, with the acquisition of a fairly dense grid (horizontal spacing of 50 and 30 meters respectively) of high-resolution seismic reflection Chirp sonar profiles with simultaneous acquisition of side scan sonar data (Figures 1, a and b).

A total of 72 sub bottom profiles lines were

recorded with a combined Chirp sonar and Side-scan sonar system Edgetech 512i (23 lines in the 2013 survey and 49 lines in the 2018 survey). The Chirp Sonar was operated in the frequency range of 0.5-7 kHz, which represents a wide-band signal with a good compromise between high resolution (~10 cm) and penetration (down to over 30m). The ship speed during acquisition was about 4–5 kn.

Seismic processing was carried out with the RadexPro software (Deco Geophysical Software CO). The processing included band-pass frequency filtering, amplitude gain correction, corrections for navigation positioning, tide correction, sensor depth correction and migration. The SEG-Y seismic data interpretation was carried out using the Kingdom Suite software (IHS Markit).

The Sidescan Sonar operated in a double frequency mode of 100kHz and 400kHz. The acquired profiles were individually processed before the creation of the seabed mosaic. The processing was carried out with the SonarWeb software (Chesapeake Technology Inc.) and included navigation corrections, removing the water column, and geometric and radiometric corrections.

The interpretation of the seismic data was carried out according to the principles of seismic stratigraphy. The main seismic sequences were identified and described considering their terminations, internal configurations and geometry. The maps presented with vertical axis in depth were calculated assuming sound speeds of 1500 m/s in the water column and 1650 m/s in the shallow unconsolidated bottom sediments.

SEDIMENT SAMPLING AND GEOTECHNICAL BOREHOLE DATA

The geological and geotechnical data used in this work consisted of sediment samples and geotechnical borehole data (Figures 1c and 1d). During the geological/geophysical surveys, 39 bottom sediment samples were collected for sediment type and grain size characterization (Figure 1d). The samples were acquired with a Petite Ponar system and then sieved through a set of meshes with different apertures. For each sample, the percentage of each of the three granulometric classes was projected in a ternary plot to classify the sediment samples according to their granulometry. Table 1 shows the granulometric classes of the sediments collected in the North Terminal.

Borehole data information used to characterize the subsurface sediments were provided by the Port of Aveiro Authority.

RESULTS

BOTTOM SEDIMENTS IN THE NORTH TERMINAL

The bottom bathymetry of the North Terminal (Figure 2), in the absence of multibeam data, was characterized by interpolating the bottom reflections interpreted in the dense grid of high-resolution seismic profiles (Figures 2a and 2b).

The bathymetry of the 2013 campaign (Figure 2a) showed that the depth varied between 3 to 14 m below water surface, but the depth remains between 9 and 11 m in most of the study area. The entrance to the North Terminal is the deepest region. Despite the low energy in the terminal area and tendency for a regular bottom, some irregularities due to prior dredging operations were observed.

The bathymetry of the 2018 campaign also presented a bottom depth between 3 to 14 m although in most of the undisturbed part of the study area the bottom depth varied between 11 to 13 m. Some bottom irregularities are probably the result of recent dredging.

The entrance of the North Terminal it is possible to visualize zones where the bottom is deeper. Although this is a region with low

energy and a tendency towards a regular bottom, some semicircular depressions are observed. The origin and distribution of these features is interpreted as pockmarks associated with gas escape to the sea bottom. It is envisaged that these structures formed by the rapid and abrupt release of gas that migrated through the sedimentary column. In Figure 2a and 2b it is possible to infer a possible west/east alignment of such structures that suggest channeling and migration of fluids through subvertical geological fault zones that can be mapped in the study area (Duarte et al., 2007). These pockmarks are also visualized on the seismic profiles, as shown in Figure 2c, above an area with acoustic blanking columns that indicate the presence of gas. The grain size of the sediments in this area showed sediments with grain sizes varying between sand and mud.

The granulometric map of the bottom sediments (Figure 3a) shows the corser sediments (sands) at the terminal entrance to the Terminal and the finer ones to the South and the East, where the currents are weaker, as expected. This progression is consistent with the area hydrodynamics, which is stronger at the entrance, attenuating towards the internal more protected parts.

The side-scan sonar mosaics allowed to obtain backscatter images of the bottom sediments and some bedforms. After processing, these mosaics allowed inferring the spatial distribution of the different sizes of bottom sediments, as they cause different levels of backscatter energy. Coarser sediments produce higher backscatter (here in brighter colors), and finer sediment produce lower backscatter (here in darker colors).

In the mosaic from the 2013 campaign (Figure 3b) three main areas can be distinguished. From west to east, a darker zone is followed by a lighter central zone and then a darker zone again. This difference in the color of the map reveals variations in the granulometry of the sediments. The map shows that the finer sediments are in the south and the eastern edge, which are the calmer areas, farther away from the entrance to the North Terminal. Coarser sediments are found at the entrance and center of the North Port Terminal, as expected. They are the first to be deposited at the entrance to the channel while the finer sediments remain in suspension and are transported to the more protected areas more distant from the terminal entrance.

Other features that can be seen in the seafloor include some furrows and some darker spots. These features are interpreted as representing records of former dredging processes carried out in the study area. As concerns a few dark spots, the Sidescan Sonar mosaic alone is not able to provide enough information to ascertain what these anomalies are. However, the presence of gas in this area is evident from the seismic data, these dark spots will likely represent pockmarks related to fluid/gas escape chimneys, forming circular or elliptical depressions. To validate these hypotheses, the bathymetry image was superimposed on the sonar mosaic (Figure 3d). It is possible to see that the depressions observed in the bathymetry coincide with the spot zones in the sonar mosaic, therefore confirming the proposed presence of pockmarks.

In the mosaic of the 2018 campaign (Figure 3b) it is possible to see that the sediments present the same behavior as in the mosaic of the 2013 campaign but clear evidence of recent dredging marks are observed.

SEISMIC STRATIGRAPHY

The high-resolution seismic data from the 2013 and 2018 campaigns from the North Terminal of the Ria de Aveiro lagoon enabled the establishment of the main depositional units. Erosive surfaces, unconformities

and correlated conformities allowed the recognition of three main seismic units: U1, U2 and U3, U3 being the most recent (Figure 4). Once the main seismic stratigraphic units were defined, it was possible to establish the various internal seismic facies. The presence of extensive acoustic anomalies (mainly acoustic blanking) masked the continuity of the reflectors.

Unit U1

The oldest unit (U1) consists of sedimentary layers, dipping to the west. Within this U1 unit, eight seismic facies (U1a, U1b, U1c, U1d, U1e, U1f, U1g and U1h) were identified, separated by surfaces with impedance contrasts. Sub-parallel internal configurations are present in all facies of the U1 unit. The upper limit of the sequence is marked by an erosive surface, with important channel incisions. The paleochannel is filled with sediment and these types of incised are normally rich in organic matter and have been considered as potential shallow methane sources.

Unit U2

The U2 lower limit is deposited in onlap against the erosive surface that marks the top of the U1 unit. The internal configuration of the U2 unit is also sub-parallel but with lower amplitude.

Unit U3

The U3 unit is the most recent and where the acoustic anomalies resulting from the presence of the gas are observed and have been mapped. Inside this unit, two distinct seismic facies (U3a and U3b) were identified, separated by a discontinuity surface. The internal configurations of the facies of the U3 unit are sub-parallel.

The available borehole data (Figure 5) allowed to infer that units U3 and U2 consist of fine, medium and even coarse sand with pebbles at depth; Unit U1 consists of consolidated clays and, according to the regional geology, this unit corresponds to the W-dipping marls, clays and limestones from the so-called "Argilas de Aveiro" (Aveiro clays) formation, of upper Cretaceous age. This unit exhibits an erosive top with channel incisions. Unit U2 and U3 consist of Quaternary sediments (Plio-Pleistocene and recent).

SHALLOW GAS ACCUMULATIONS

The geophysical surveys allowed the identification and mapping of several gas accumulations (Figures 4 to 6). The sedimentary layers on the high-resolution seismic reflection profiles show interruptions marked by acoustic blanking and/or turbidity, indicative of gas presence.

The presence of gas in the sedimentary pores results in the absorption of the seismic energy and this produces a blanking zone that masks the existing reflections (Judd and Hovland, 1992). The presence of acoustic turbidity was observed in all seismic profiles from the two geophysical surveys carried out in the study area (e.g., Figure 6).

The acoustic turbidity zones have very diffuse upper limits but are generally marked by discontinuous and high amplitude reflections. Their lateral terminations are well defined, clearly showing the gas zones and acoustic windows within the sedimentary layers. The areas with gas accumulations in the North Terminal occur within the limits of the sedimentary units U3 and U2 (Figure 6).

Gas accumulations in the studied area occur at a depth ranging from 0.5 m to 3 m below the bottom. The campaigns of 2013 and 2018, in spite of their differences in line spacing, appear to indicate an increase in the gas fields from 0.22 Km^2 to 0.34 Km^2 respectively in this 5-year period (Figure 7).

Acoustic plumes could also be observed as anomalies in the water column indicating gas leakage. These anomalies consist of reflections caused by the large differences in acoustic impedance between free gas and water

(Addy and Worzel, 1979). Acoustic plumes in the water column were observed in several seismic profiles of the north port terminal (Figure 8), above or close to areas in which the seismic profiles reveal the presence of gas accumulations. Lower hydrostatic pressure at low tide in the shallower regions reduces methane solubility causing an increase in the volume of free gas in sediment, causing gas bubbles to escape from the sediment (Lee et al., 2005).

DISCUSSION

The presence of gas in the sediments has a significant effect on the geoacoustic behavior. The accumulations reported here were identified as anomalous or chaotic low amplitude reflections often marked at the top by a strong reflector. In all seismic sections in the studied area, well defined sectors with this character interrupt the continuity of the reflections from the underlying geology due to seismic energy absorption by the gas accumulations. The gas bubbles strongly scatter the acoustic energy of the high-frequency seismic source, and the significantly higher attenuation due to bubble resonance will further prevent transmission through the gas-charged sediment layer. The resulting appearance of the shallow gas accumulations on the data, as observed in Figure 4, are characterized by acoustic turbidity and acoustic blanking, that mask the underlying geology.

The distribution of the gas accumulations indicates that the facies that cover them are impermeable or semi-permeable layers that behave like a seal, forcing a horizontal flow with lateral extensions. These anomalies have a different morphology for gas in sediments and gas leakage in the water allowing mapping. These gas accumulations all occur in the Quaternary sedimentary layers.

The gas front lies between 0,5 and 3 m below the seabed and marks the transition from gas in the dissolved phase to bubble phase when the gas concentration exceeds the saturation level.

The general facies succession registers a general transgression since the LGM (last glacial maximum), in which the coastline shift was controlled by the interaction between global (sea level rise, climate) and regional factors. The stratigraphic analysis allows to establish a relationship between the relative changes in sea level during late Pleistocene and Holocene, which determine the morphology of the bottom of both estuaries. Sea level was the most relevant control factor that determined sedimentary filling, according to the analyzed seismic data. During the Last Glacial Maximum Stadial (Marine Isotope Stage 2 - MIS 2), the sea level reached a position approximately 120 to 130 m below the current level (Dias et al., 2000), with the exposure of the oldest sedimentary units. The presence of paleochannels in some profiles is clear evidence of the fluctuations that occurred during the Quaternary period, demonstrating this exposure phase. Some gas occurrences in the study area occur just above some of these channels, as can be seen in Figure 4a. Since the end of the last Pleistocene glaciation, the sea level has risen, initiating a transgression that marked the beginning of the Holocene. During sea level rise, after the last glaciation (Bard et al., 1990), depositional and erosional processes resulted in the observed morphological features associated with past channels.

The three sequence boundaries proposed by Meyers and Milton (1996), i.e. erosional surface, transgressive surface and maximum flooding surface are all recognized in the high-resolution seismic data acquired.

The geological environment suggests that the gas likely has a biogenic genesis derived from the accumulation of organic matter

and associated with sediments deposited during the Holocene TST (Transgressive System Tract) and HST (Highstand System Tract). The organic material is degraded by bacteria, forming basically methane. A rapid sedimentation rate can lead to the burial, accumulation, and preservation of this gas. The distribution of sedimentary facies, in turn, influences the processes of gas generation, migration and accumulation, as well as the areas in which methane escapes from the sediments into the water layer, forming flares (Figure 8).

The gas accumulations are also likely related to oceanographic and geomorphological conditions. The hydrodynamic regime helped in the sedimentation of fine materials and, consequently, the formation of seals that trap the gas upward migration and its accumulation.

In the North Terminal area, the variation in hydrostatic pressure due to the difference in water mass due to the tidal cycle (maximum variation of 3m, which is significant considering the shallow depths in the study area) appears to enhance the gas-related reflections and promote the gas release into the water layer, as demonstrated by Duarte et al., 2007). The comparison of seismic profiles acquired at different tidal altitudes revealed that the acoustic detection of gas in the sediments and gas leaks in the water column of the North Port Terminal of the Ria de Aveiro is influenced by tides. Amplitudes and size of the strongest and largest signals are observed in profiles acquired during low tide. This is because a better detection of gas bubbles occurs when hydrostatic pressure and lower salinity result in variations in bubble size.

CONCLUSIONS

The acquisition and analysis of the geophysical and geotechnical data has allowed recognition the superficial stratigraphy and gas accumulations of the North Port Terminal at Ria de Aveiro lagoon.

In the study area, three seismic units have been identified: Unit 1 (U1), interpreted as "Aveiro clays" of Upper Cretaceous age, with an erosive top and paleochannel incision; two Quaternary units (U2 and U3) correlated with late Pleistocene and Holocene post-glacial sedimentation, the boundaries of which have defined as resulting from sea level changes that mainly occurred during the late Quaternary.

The results obtained with this high-resolution seismic study have shown that the dense grid of seismic data enabled the detailed mapping of seismic evidence of gas accumulation and seepage. The gas has a significant effect on the geoacoustic behavior of the sedimentary package. The observed acoustic masking is attributed to the presence of gas bubbles (predominantly free methane gas) in the sediments. Gas charged sediment attenuates the acoustic energy and limits the subbottom penetration thereby masking all underlying stratigraphic features (Hovland and Judd, 1988, Judd and Hovland, 1992; Judd and Hovland, 2007).

The observed gas signatures include acoustic turbidity and blanking in the subsurface, pockmarks in the bottom, and acoustic plumes in the water column. In the North Terminal of the Ria de Aveiro port area, when comparing the data from the geophysical campaigns of 2013 and 2018, there is a suggestion that the area of gas fields have increased during this period, from ca. 0.22 km^2 to 0.34 km^2.

Gas-rich sediments are associated with late Pleistocene and Holocene facies rich in organic matter. This gas was generated from the degradation of the organic matter

accumulated in the period of exposure and buried, during the TST and during the Holocene HST.

The Quaternary sedimentary succession can be summarized as a transition from fluvial deposits, followed by nearshore to shoreface sediments, and finally capped by marine; successive cycles of sea level fall/rise caused erosion and reworking of these deposits.

It is hoped that this study contributes to a better knowledge of the sub-bottom geology, seismic stratigraphy and gas accumulations in this area of the Ria of Aveiro, and also allow for a better planning of future dredging operations in this area. Since these dredging operations are recurrent, a better knowledge of the sub-bottom geology and the location of areas os shallow gas accumulation is essential.

ACKNOWLEDGEMENTS

The authors thank the colleagues from the Marine Geology and Geophysics Laboratory Clara Sena, Bernardo Azevedo, and Ana Margarida Carvalho for useful discussions and support. This research was supported by the National Council for Scientific and Technological Development (CNPq / BR), the Portuguese Foundation for Science and Technology (FCT), and the Center for Environmental studies and the Sea (CESAM). Thanks also to the Administration of the Harbor of Aveiro (APA) and the University of Aveiro. (Veja por favor com a Dra. Ana Sofia Santiago do CESAM, qual é o texto pelo CESAM que tem que ser incluído).

REFERENCES

Addy S. K. and Worzel J. L., 1979. Gas seeps and subsurface structure of Panama City, Florida Am, Assoc. Petrol Geo. Bull. 63, 668-675.

Bard E., Hamelin B., Fairbanks R.G., 1990. U-Th Ages obtained by mass spectrometry in corals from Barbados: Sea Level During the Past 130,000 Years. Nature, 346, 456-458.

Dias J.M., Lopes J.F, Dekeyser I., 2000. Tidal propagation in Ria de Aveiro Lagoon, Portugal. Phys Chem Earth, B Hydrol Oceans Atmosphere 25(4):369–374.

Duarte H., Parsons B., Pinheiro L.M., Rodrigues A., Bernardes C., Rosa L., 2003. Bottom features in the Ria de Aveiro (Portugal) revealed by Side-Scan Sonar Imaging. In: Abstract Vol 4th Symp Atlantic Iberian Continental Margin, Vigo. Thalassas, 39–40.

Duarte H., Pinheiro L.M., Teixeira F.C.E, Monteiro J.H., 2007. High-resolution seismic imaging of the methane gas and gas seepage in the sediments of the Ria de Aveiro (Portugal). Geomarine Letters, Doi 10.1007/S00367-007-0069-Z.

Faria J.B., Zbyszewski G., Jesus T.A., 1967. O aparecimento de gás na Gafanha da Boa Hora (Vagos). Bol. Minas Lisboa 4 (2):125–130 (in Portuguese).

Fleischer P., Orsi T.H., Richardson M.D., Anderson A.L., 2001. Distribution of free gas in marine sediments: A Global Overview. Geo Mar Lett 21:103–122.

Floodgate G.D., Judd A.G., 1992. The origins of shallow gas. Continental Shelf Research 12 (10), 1145–1156.

Garcia-Garcia A., Orange D.L., Miserocchi S., Correggiari A., Langone L., Lorenson T.D., Trincardi F., Nittrouer C.A., 2007. What controls the distribution of shallow gas in the Western Adriatic Sea? Continental Shelf Research 27(3/4), 359-374.

Garcia-Garcia A., Vilas F., Garcia-Gil. S., 1999. A seeping sea-floor in ria environment: Ria de Vigo (Spain). Environment Geology, 38(4):296-300.

García-Gil S., 2003. A natural laboratory for shallow gas: The Rias Baixas (Nw Spain). In: Woodside Jm, Garrison Re, Moore Jc, Kvenholden Ka (Eds) Proc 7th Int Conf Gas in Marine Sediments, 7–12 October 2002, Baku, Azerbaijan. Geo-Mar Lett 23(3/4):215–229.

García-Gil S., Vilas F., García-García A., 2002. Shallow gas features in incised-valley fills (Ria de Vigo, Nw Spain): A Case Study. Cont Shelf Res 22(16):2303–2315.

Hovland M., Judd A.,1988. Seabed pockmarks and seepages. impact on geology, biology and the marine environment. Graham and Trotman, London.

Hovland M., Judd A.G., 1992. The global production of methane from shallow submarine sources. Cont. Shelf Res.12, 1231-1238.

Iglesias J., García-Gil S., 2007. High-Resolution mapping of shallow gas accumulations and gas seeps in San Simon Bay (Ría de Vigo, Nw Spain). Some Quantitative Data. Geo- Marine Letters 27, 103–114.

Judd A.G., Hovland M., 2007. Seabed fluid flow: the impact on geology, biology and the marine environment. Cambridge University Press, New York.

Judd A.G., Hovland M., 1992. The evidence of shallow gas in marine sediments. Cont. Shelf Res. 12, 1081–1095.

Karisiddaiah S.M., Veerayya M., Vora K.H., Wagle B.G., 1992. Gas-charged sediments on the inner continental shelf off Western India. Marine Geology, 110:143-152.

Kelley C.A., Martens C.S., Ussler W., 1995. methane dynamics across a tidally flooded riverbank margin. Limnol Oceanography 40(6):1112–1129.

Lee, G.H., Kim, D.C., Kim, H.J., Jou, H.T., Lee, Y.J., 2005. Shallow gas in the central part of the Korea strait shelf mud off the Southeastern Coast of Korea. Continental Shelf Research 25, 2036-2052.

Martínez-Carreño N., García-Gil S., 2013. The Holocene gas system of the Ria De Vigo (Nw Spain): Factors controlling the location of gas accumulations, seeps and pockmarks. Mar. Geol. 344, 82–100.

Meyers K.J., Milton N.J., 1996. Concepts and principles of sequence stratigraphy. In Emery, D., Meyers, K.J. (Eds.), Sequence Stratigraphy. Blackwel Science, London, 296 pp.

Missiaen T., Murphy S., Loncke L., Henriet J.P., 2002. Very high-resolution seismic mapping of shallow gas in the Belgian coastal zone. Continental Shelf Research (2002), Vol. 22, N° 16, P.P. 2291-2301 (11).

Okyar M., & Ediger V., 1999. Seismic evidence of shallow gas in the sediment on the shelf off Trabzon, Southeastern Black Sea. Continental Shelf Research (1999), Vol. 19, N° 5, P.P. 575-587 (13).

Papatheodorou G., Hasiotis T., Ferentinos G., 1993. Gas-charged sediments in the Aegean and Ionian Seas, Greece. Marine Geology, 112:171-184.

Park S.C., Kim Y.S., Hong S.K., 1991. Shallow seismic stratigraphy and distribution pattern of late quaternary sediments in a macrotidal bay, Gunhung Bay, West Coast of Korea. Marine Geology, 98:135-144.

Schroot B.M., Schüttenhelm R.T.E., 2003. Shallow gas and gas seepage: expressions on seismic and other acoustic data from the Netherlands North Sea. J. Geochem. Explor. 78–79, 305–309.

Teixeira S., 1994. Morphosedimentary dynamics of the Ria de Aveiro (Portugal). University of Lisboa, Lisboa, Pp 1–378.

Teixeira C., & Zbyszewski G., 1976. Notícia Explicativa Da Folha 16-A, Aveiro. Carta Geológica De Portugal Na Escala De 1/50.000. Lisboa, Serviços Geológicos De Portugal.

Terra L.C., Calliari L.J., Griep G.H., 2014. Acumulações de gás nos sedimentos da plataforma continental interna do Rio Grande Do Sul. In. VI Simpósio Brasileiro de Geofísica. Porto Alegre, RS. 3p

Van Der Nat F.J., Middelburg J.J., 2000. Methane emission from tidal freshwater marshes. Biogeochemistry 49(2):103–121

Weschenfelder J., Klein A.H.F., Green A.N., Aliotta S., Mahiques M.M., Neto A.A., Terra L.C, Corrêa I.C.S., Calliari L.J, Montoya I., Ginsberg S.S., Griep G.H., 2016. The control of palaeotopography in the preservation of shallow gas accumulation: examples from Brazil, Argentina and South Africa, Estuarine, Coastal and Shelf Science, V. 172, 93–107.

Zhou H., Yin X., Yang Q., Wang H., Wu Z., Bao S., 2009. Distribution, source and flux of methane in the Western Pearl River Estuary and Northern South China Sea. Marine Chemistry, 117(1-4), 21–31.

Name	Year	UTM X	UTM Y	Depth Z (m)	Granul Class
TN1-01	2013	523271,60	4500284,90	13.5	Clayey sand
TN1-02	2013	523422,65	4500103,88	13.7	Clayey sand
TN1-03	2013	523431,88	4500126,11	13.9	Clayey sand
TN1-04	2013	523171,89	4499555,85	12.5	mud
TN1-05	2013	523281,57	4499457,45	13,00	mud
TN1-06	2013	523889,54	4500288,73	13.5	mud
TN1-07	2013	524014,96	4500253,44	13,00	mud
TN1-08	2013	524102,84	4500319,04	14,00	mud
TN1-09	2013	524131,38	4500183,95	14,00	mud
TN2-01	2014	522945,66	4500017,67	10,00	muddy sand
TN2-02	2014	522966,43	4499932,68	11.5	muddy sand
TN2-03	2014	523299,81	4500182,06	15,00	muddy sand
TN2-04	2014	523300,13	4500079,53	13,00	muddy sand
TN2-05	2014	523372,62	4500209,63	12,00	muddy sand
TN2-06	2014	523381,05	4500187,63	14.5	muddy sand
TN2-07	2014	523383,02	4500043,34	13,00	muddy sand
TN2-08	2014	523387,73	4499993,99	12.5	muddy sand
TN2-09	2014	523392,73	4500096,53	12.5	muddy sand
TN2-10	2014	523446,66	4500093,66	12.5	muddy sand
TN2-11	2014	523457,92	4500132,43	13,00	muddy sand
TN2-12	2014	523469,58	4500048,17	12.5	muddy sand
TN2-13	2014	523481,96	4500215,29	12.5	muddy sand
TN2-14	2014	523487,39	4500181,13	12,00	muddy sand
TN2-15	2014	523588,01	4500063,73	12.5	muddy sand
TN2-16	2014	522939,29	4500112,59	11.5	sand
TN2-17	2014	523090,17	4500192,79	12,00	sand
TN2-18	2014	523113,10	4500146,54	11,00	sand
TN2-19	2014	523270,08	4500215,38	11.5	sand
TN2-20	2014	523058,16	4499983,85	10,00	sandy mud
TN2-21	2014	523321,31	4499863,91	12,00	sandy mud
TN2-22	2014	523472,26	4499921,35	12,00	sandy mud
TN2-23	2014	523506,94	4500003,48	12,00	sandy mud
TN2-24	2014	523703,77	4500200,04	13,00	sandy mud
TN2-25	2014	523085,25	4499853,84	12.5	Sandy silty clay
TN2-26	2014	523458,10	4500123,08	14.1	Sandy silty clay
TN2-27	2014	523738,26	4500022,40	11.1	Sandy silty clay
TN2-28	2014	523849,74	4500322,03	14.2	Sandy silty clay
TN2-29	2014	523902,67	4500164,02	14.2	Sandy silty clay
TN2-30	2014	523907,88	4500119,52	15.9	Sandy silty clay

Table 1 - Granulometric data collected in Terminal Norte during the two surveys, in October of 2013 and March of 2014.

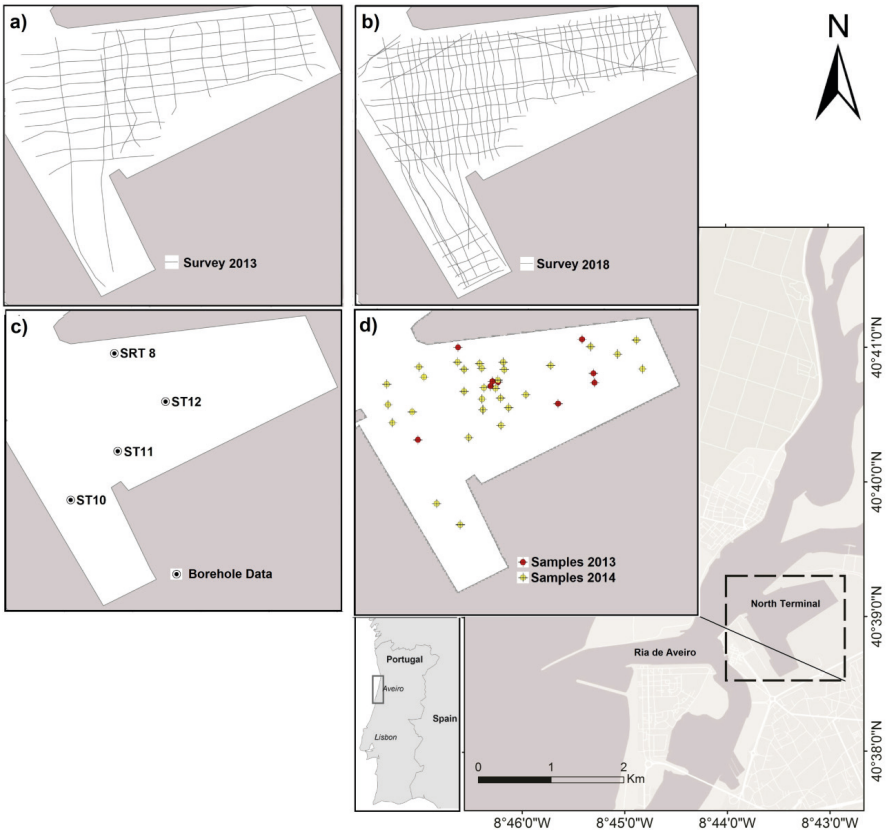

Figure 1 – Location of the North Terminal of the Port of Aveiro, in the Ria de Aveiro barrier/lagoon system, showing the location of the seismic profiles, sediment samples and geotechnical boreholes: a) seismic lines acquired in the 2013 geophysical campaign; b) seismic lines acquired in the 2018 geophysical campaign; c) existing boreholes; d) sediment samples collected during the 2013 and 2014 campaigns.

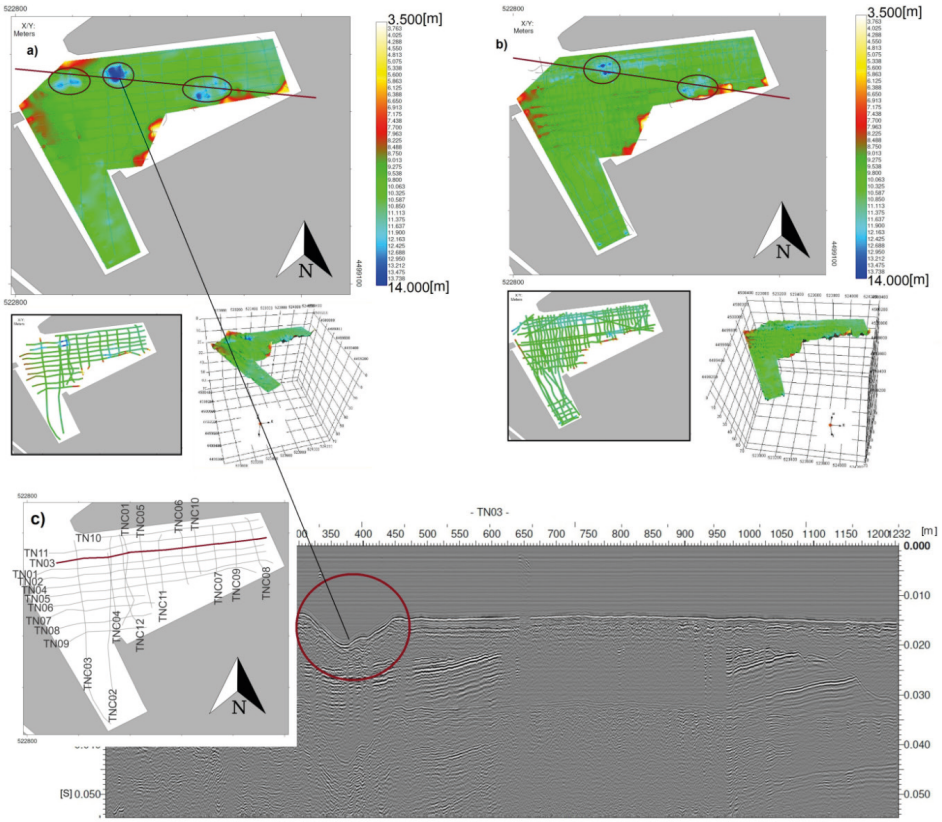

Figure 2 – a) Bathymetry of the North Port Terminal interpolated from the 2013 seismic survey; b) bathymetry of the North Port Terminal interpolated from the 2018 seismic survey; c) TN10 seismic Profile from the 2013 geophysical campaign showing semicircular depressions in the bottom topography which are interpreted as pockmarks, resulting from gas escape (gas columns are seen below the depression in the seismic line).

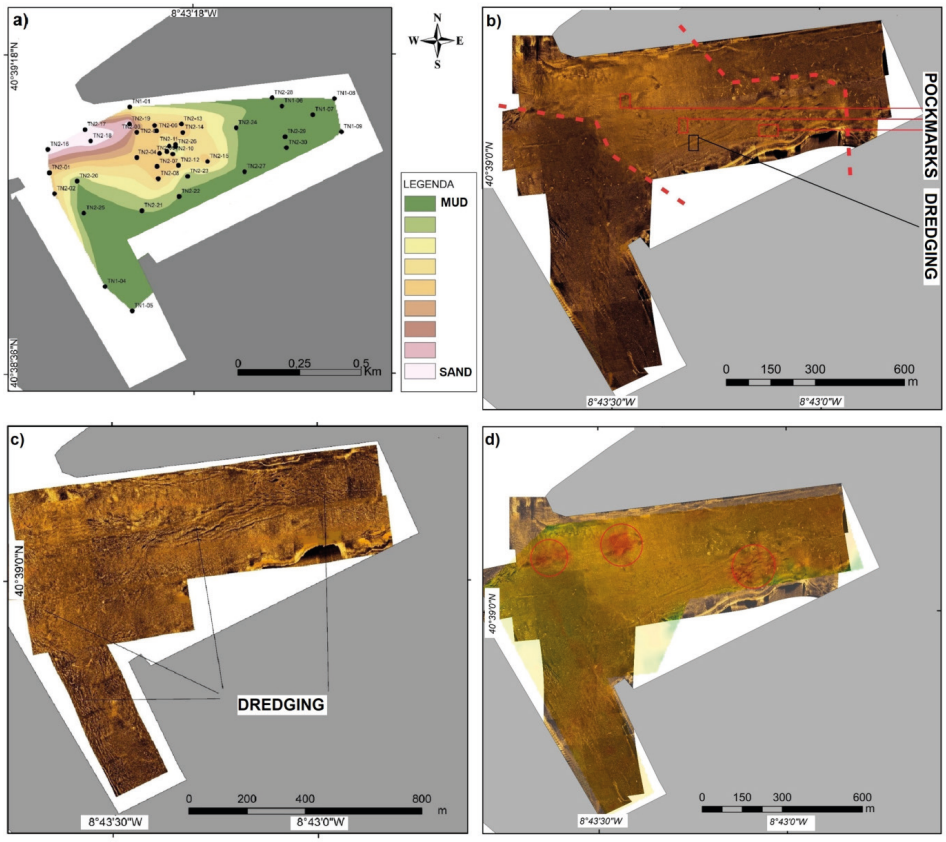

Figure 3 – a) Interpolated granulometric map of from the sediment samples from the lagoon bottom of the North Port Terminal, assuming no major changes in sediment type occurred between the two surveys; b) Sidescan sonar mosaic from the 2013 geophysical survey; c) Sidescan sonar mosaic from the 2018 geophysical survey; d) Sidescan sonar mosaic from the 2013 geophysical campaign with the corresponding bathymetric map overlayed on top of it. In red zone, coincident structures interpreted as related to gas escape are observed.

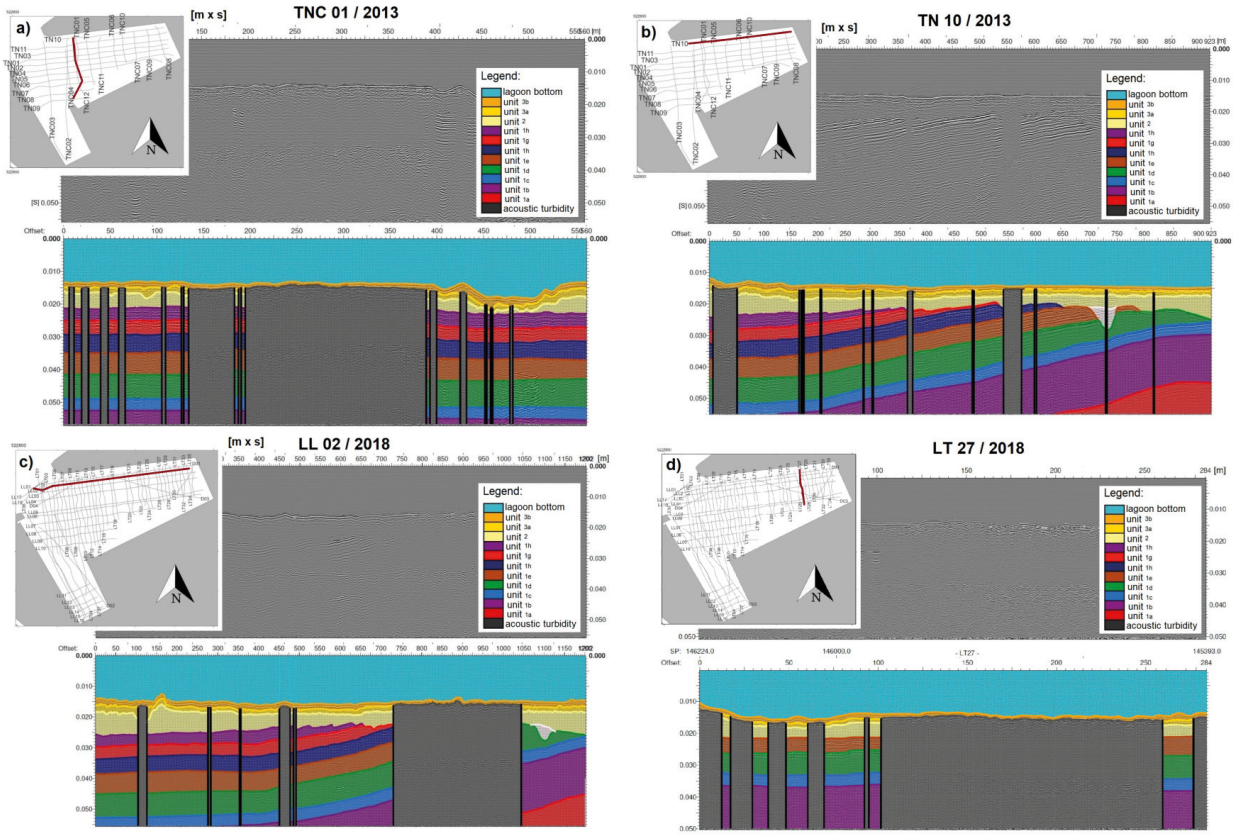

Figure 4 – a) Seismic profile TNC 01 from the 2013 geophysical survey; b) seismic profile TN10 from the 2013 geophysical survey; c) seismic profile LL02 from the 2018 geophysical survey; d) seismic profile LT27 from the 2018 geophysical survey.

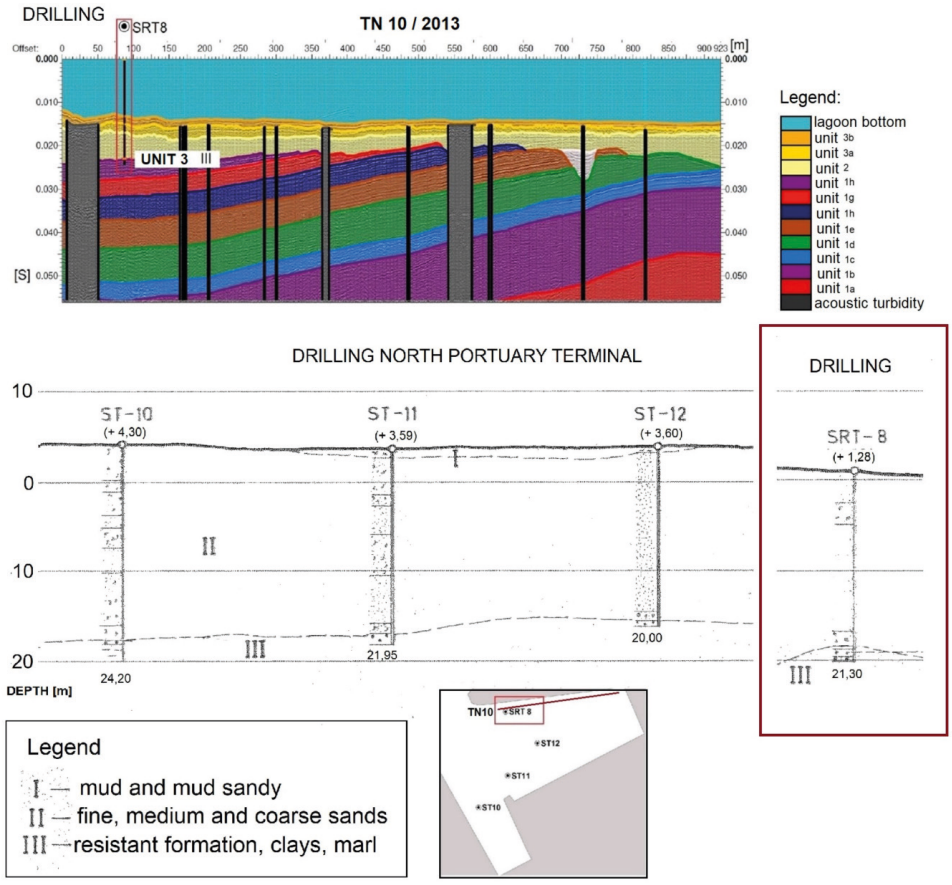

Figure 5 – Borehole data from the study area (SRT8, ST12 ST11 and ST10) and their interpretation.

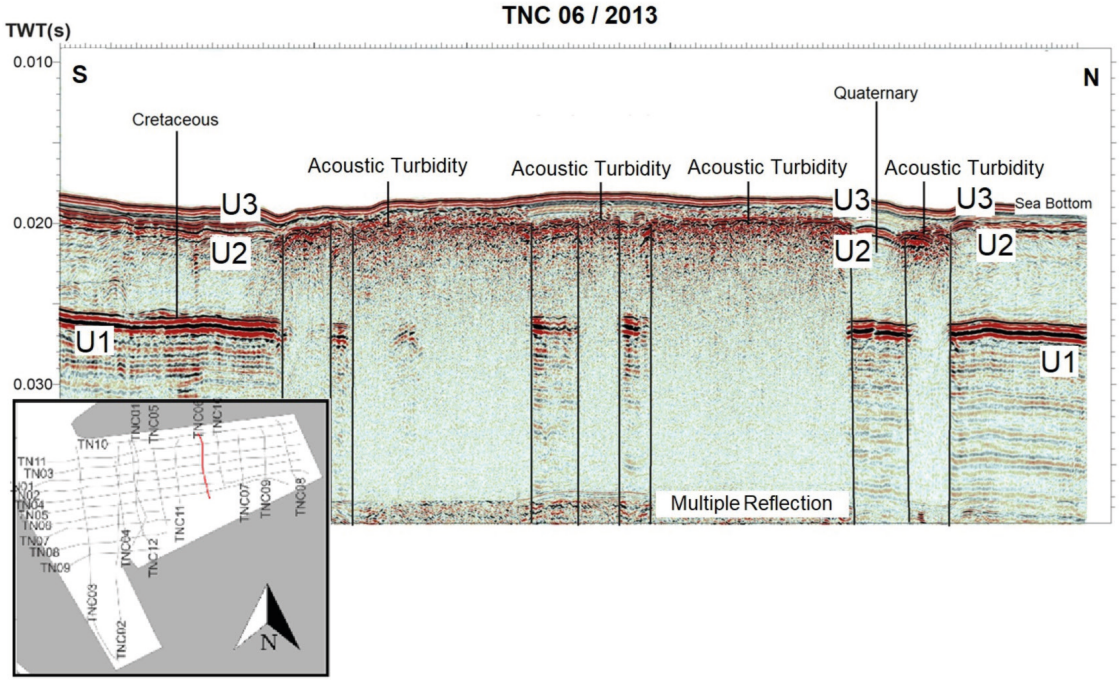

Figure 6 – Seismic profile TNC 06 of the North Port Terminal of the 2013 geophysical survey.

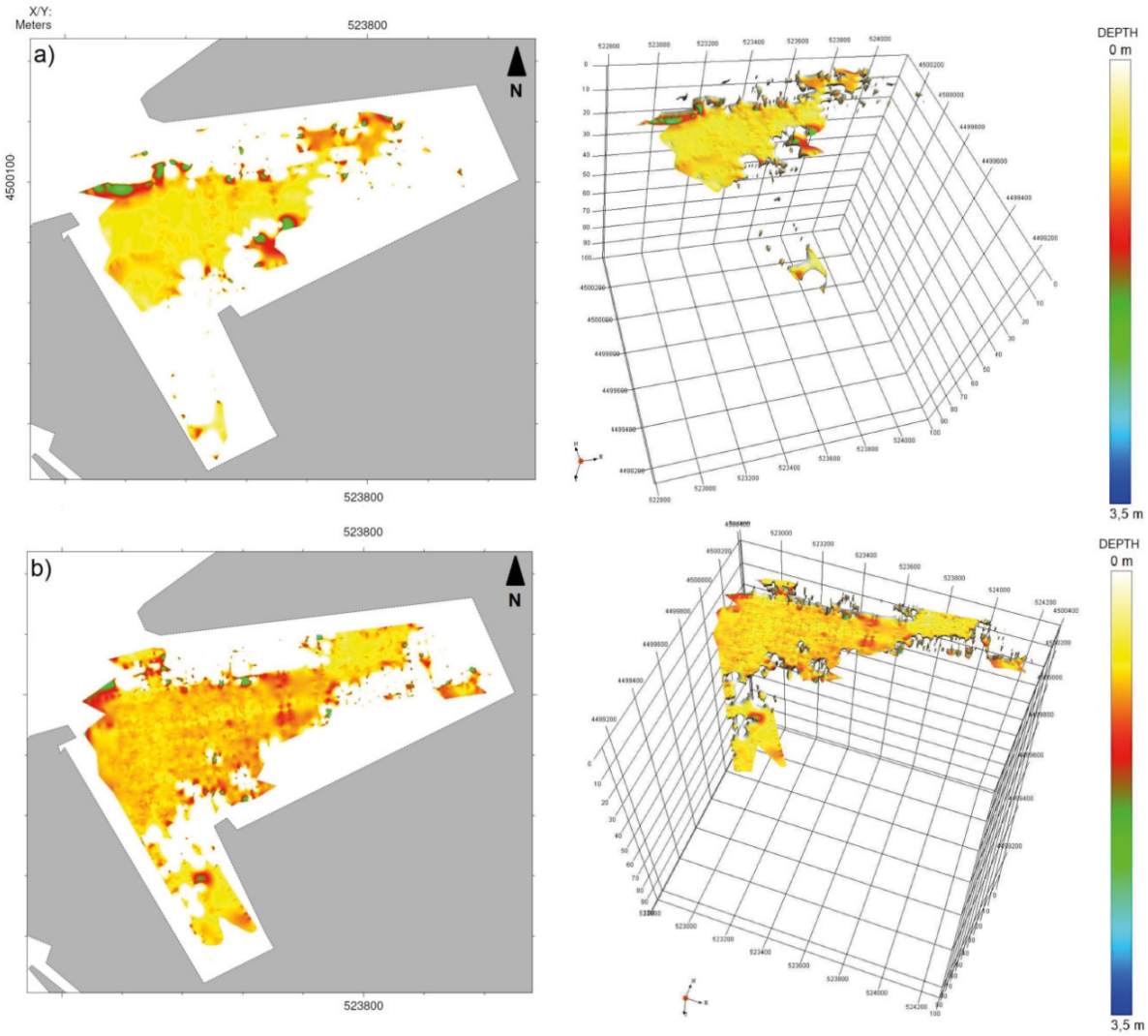

Figure 7 – Gas location maps in the North Port Terminal: a) data from the 2013 geophysical campaign; b) data from the 2018 geophysical campaign.

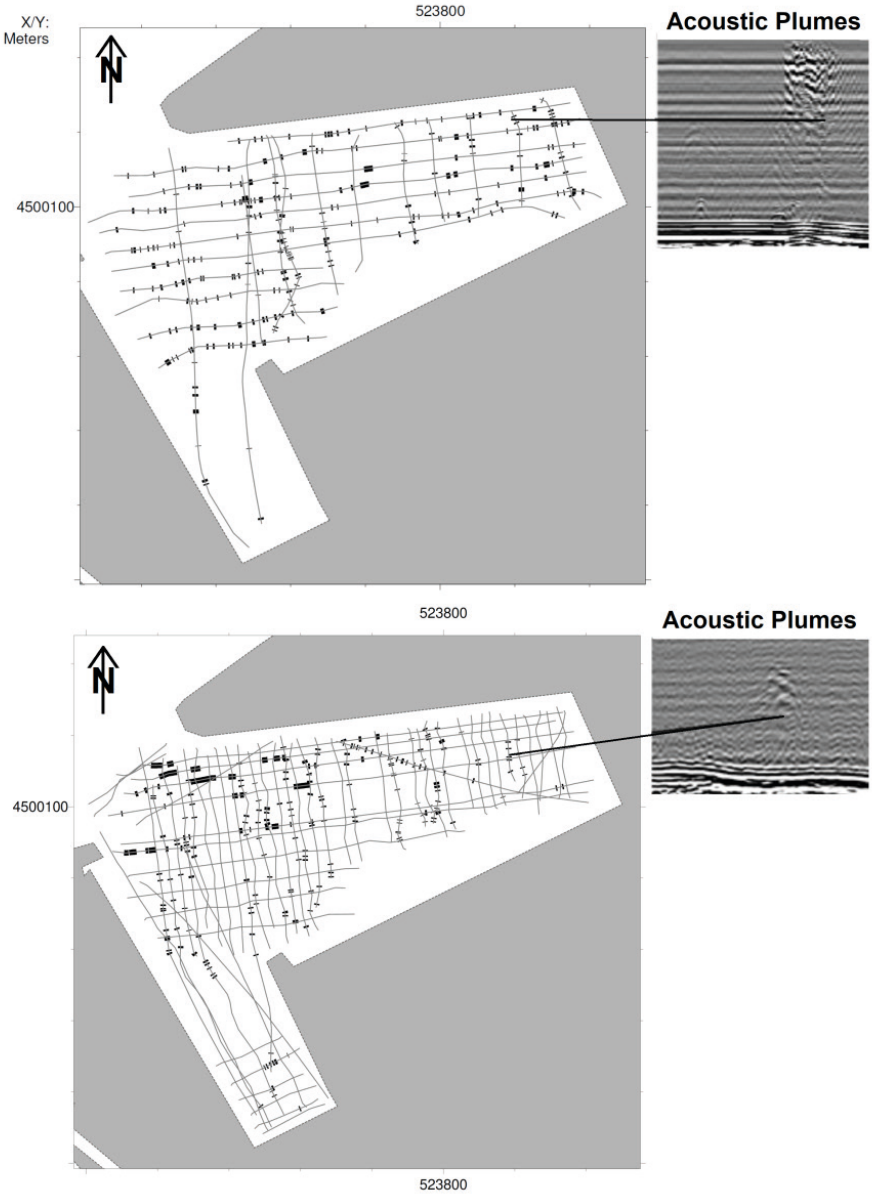

Figure 8 – Maps of Acoustic Plumes in the water column of the North Terminal: a) 2013 seismic survey, b) 2018 seismic survey.